JOURNAL OF VIROLOGY, Dec. 2010, p. 12862–12871 Vol. 84, No. 24
0022-538X/10/$12.00 doi:10.1128/JVI.01478-10


# Fitness Disadvantage of Transitional Intermediates Contributes to Dynamic Change in the Infecting-Virus Population during Coreceptor Switch in R5 Simian/Human Immunodeficiency Virus-Infected Macaques[▽]

Madina Shakirzyanova, Wuze Ren, Ke Zhuang, Silvana Tasca, and Cecilia Cheng-Mayer*

*Aaron Diamond AIDS Research Center, New York, New York*

Received 14 July 2010/Accepted 30 September 2010

**Fitness disadvantage of the transitional intermediates compared to the initial R5 viruses has been suggested to constitute one of the blockades to coreceptor switching, explaining the late appearance of X4 viruses. Using a simian model for human immunodeficiency virus type 1 (HIV-1) coreceptor switching, we demonstrate in this study that similar molecular evolutionary pathways to coreceptor switch occur in more than one R5 simian/human immunodeficiency virus (SHIV)$_{SF162P3N}$-infected macaque. In infected animals where multiple pathways for expansion or switch to CXCR4 coexist, fitness of the transitional intermediates in coreceptor usage efficiency influences their outgrowth and representation in the infecting virus population. Dualtropic and X4 viruses appear at different disease stages, but they have lower entry efficiency than the coexisting R5 strains, which may explain why they do not outcompete the R5 viruses. Similar observations were made in two infected macaques with coreceptor switch, providing *in vivo* evidence that fitness disadvantage is an obstacle to X4 emergence and expansion.**

Entry of the human immunodeficiency virus type 1 (HIV-1) requires interactions between the viral envelope glycoprotein and cell surface CD4 and a chemokine receptor, either CCR5 or CXCR4 (4). Most HIV transmissions are initiated with CCR5-using (R5) viruses. However, in nearly half of treatment-naïve HIV-1 subtype B-infected individuals, variants that use CXCR4 (X4) arise late in infection, and their emergence is associated with accelerated $CD4^+$ T cell loss and rapid disease progression (3, 9, 13, 33, 46, 47, 55, 56). The R5-to-X4 evolutionary process *in vivo* and *in vitro* transitions through intermediates that are able to use both coreceptors (13, 46, 51) and requires amino acid changes in the V3 loop of envelope glycoprotein gp120 (26). However, while the genotypic and phenotypic determinants for expansion or switch to CXCR4 use are well characterized, the mechanistic basis and obstacles for change in coreceptor preference *in vivo* are yet to be fully elucidated. Among several factors that have been proposed as playing important roles, fitness disadvantage of the transitional intermediates compared with the initial R5 viruses has been suggested to constitute one of the blockades to coreceptor switching (34, 42), explaining the late appearance of X4 viruses.

We recently developed an R5 simian/human immunodeficiency virus (SHIV)$_{SF162P3N}$ infection of a rhesus macaque model to study coreceptor switch *in vivo* (27, 28, 43). The macaques infected intravenously (i.v.) or intrarectally (i.r.) with R5 SHIV$_{SF162P3N}$ in which X4 virus evolved and emerged are rapid progressors (RPs), with a clinical course that is characterized by extremely high levels of virus replication and weak or undetectable antiviral antibody and cellular immune responses. We demonstrated that, similar to findings in humans (11, 15, 20, 31, 49, 52), sequence changes in the V3 loop of envelope gp120 determine the phenotypic change from R5 to X4 in macaques. Furthermore, consistent with reports for HIV-1-infected individuals (7, 8), the newly emerging CXCR4-using viruses in infected macaques are highly sensitive to neutralization with soluble CD4 (sCD4), and their emergence follows rather than precedes the onset of precipitous $CD4^+$ T cell loss. Given that the conditions (e.g., extremely high levels of virus replication), genotypic requirements (i.e., V3 loop sequence changes), and pattern (e.g., emergence of neutralization-sensitive X4 variants following the onset of $CD4^+$ cell loss) for coreceptor switching in SHIV$_{SF162P3N}$ i.v.- and i.r.-infected macaques overlap with those reported for humans, this model will be highly useful in studies to understand the underlying selection pressures, obstacles, and envelope evolutionary processes for tropism change *in vivo*.

With regard to the obstacles and pathway of phenotypic switch, we previously reported that the earliest X4 viruses in the i.v.-infected macaque BR24 also retained CCR5 usage (54). In contrast to the final X4 variant, the dualtropic R5X4 virus had insertions of amino acids histidine and isoleucine (HI) instead of histidine and arginine (HR) upstream of the GPG crown of the V3 loop (Table 1). Moreover, compared to the inoculating R5 and the final X4 viruses, the dualtropic intermediate virus has reduced replicative capacity and decreased CCR5 and CXCR4 usage efficiency, suggestive of fitness disadvantage. CA28, another i.v.-infected RP macaque with coreceptor switch, took a different pathway to acquire CXCR4 use, requiring mutations of the GPG crown sequence in the V3 loop to RRW in conjunction with an alanine deletion downstream of the crown (designated RRW.A) (Table 1). This X4 variant first appeared in CA28 at 11 weeks postinfection

* Corresponding author. Mailing address: Aaron Diamond AIDS Research Center, 455 First Avenue, 7th Floor, New York, NY 10065. Phone and fax: (212) 448-5080. E-mail: cmayer@adarc.org.
▽ Published ahead of print on 13 October 2010.

TABLE 1. Clinical history, V3 sequence, and phenotypic characterization of tropism intermediates previously reported[a]

| Macaque | Route of infection | Clinical course | Variant | Time of emergence | CD4 T-cell count[b] | V3 loop sequence | Phenotype | Reference |
|---|---|---|---|---|---|---|---|---|
| BR24 | i.v. | RP | HI | 20 wpi | 229 | CTRPNNNTRKSIRI**HI**GPGRAFYATGDIIGDIRQAHC | R5X4 | 54 |
| | | | HR | 20 wpi | 229 | -----Y-I------**HR**---------- | X4 | |
| CA28 | i.v. | RP | RRW.A | 11 wpi | 237 | ----------H-..**RRW**-.---------- | X4 | 28 |
| DG08 | i.r. | RP | Δ22-25 | 13 wpi | 314 | ---------R--H-..-------....---------- | Dual-R | 43 |
| | | | HR | 13 wpi | 314 | ----------**HR**---------- | X4 | |

[a] i.v., intravenous; i.r., intrarectal; RP, rapid progressor; wpi, weeks postinfection. For V3 sequence, dots indicate gaps and dashes stand for identity in sequences. Amino acid residues conferring CXCR4 usage are in bold type.
[b] CD4 T cell count (per μl blood) at time of tropism variant emergence.

(wpi), but whether the switch event transitions through intermediates that are less fit but can use CXCR4 in addition to CCR5 was not investigated.

X4 variants with HR insertions in the V3 loop were also found in the i.r.-infected macaque DG08 near end-stage disease (43). In addition to this evolutionary pathway, however, phylogenetically distinct variants that harbored four amino acid deletions in the C-terminal stem region of the V3 loop (ATGD; designated Δ22-25) and that preferred CCR5 over CXCR4 were also found in DG08 (Table 1). Such tropism variants have been described in HIV-1-infected individuals (22, 30) and are classified as dual-R. Interestingly, clonal analysis of tissue envelope sequences suggested that the dual-R Δ22-25 switch event took place earlier than the X4 HR switch. However, over time, the frequency of the dual-R variant decreased while that of the X4 HR virus increased. To explain this change in virus population during coreceptor switch, we hypothesized that although the dual-R Δ22-25 variant may have had a distinct advantage over earlier or coexisting R5 viruses when it first appeared because of target cell expansion through acquisition of CXCR4 usage, this advantage was lost with the subsequent emergence of the X4 variant that uses CXCR4 more efficiently, accounting for its diminished dominance with time. We tested this hypothesis in the present study by comparing CCR5 and CXCR4 usage efficiency, as well as entry fitness of the coevolving R5, dual-R, and X4 viruses in DG08. We further sought to identify transitional intermediates in macaque CA28 to determine if similar costs and benefits are associated with coreceptor switching in this animal. Our goal is to better understand the molecular evolutionary pathways and blockade(s) to phenotypic switch for R5 $SHIV_{SF162P3N}$ and the properties of the transitional intermediates that allow them to eventually outgrow and amplify.

## MATERIALS AND METHODS

**Cell culture.** Rhesus peripheral blood mononuclear cells (RhPBMC) were obtained by Ficoll-Hypaque gradient purification followed by stimulation with 3 μg/ml staphylococcus enterotoxin B (SEB) (Sigma-Aldrich, St. Louis, MO) in RPMI 1640 medium supplemented with 10% fetal bovine serum (FBS), 2 mM glutamine, 100 U/ml penicillin, 100 μg/ml streptomycin, and 20 U/ml of interleukin-2 (IL-2) (Novartis, Emeryville, CA). 293T cells and TZM-bl cells expressing CD4, CCR5, and CXCR4 and containing integrated reporter genes for firefly luciferase and β-galactosidase under the control of the HIV-1 long terminal repeat (LTR) (58) were maintained in Dulbecco modified Eagle medium (DMEM) supplemented with 10% FBS, penicillin, streptomycin, and L-glutamine. U87 cells stably expressing CD4 and one of the chemokine receptors (17) were maintained in DMEM supplemented with 10% FBS, antibiotics, 1 μg/ml puromycin (Sigma-Aldrich), and 300 μg/ml G418 (Geneticin; Invitrogen, Carlsbad, CA).

**DNA, RNA extraction, sequencing, and analysis.** Proviral DNA was extracted from $3 \times 10^6$ infected macaque PBMC or tissue cells with a DNA extraction kit, and viral RNA was prepared from 500 μl plasma using a commercially available RNA extraction kit (Qiagen, Valencia, CA) followed by reverse transcription with Superscript III reverse transcriptase (RT) (Invitrogen, Carlsbad, CA) and random hexamer primers (Amersham Pharmacia, Piscataway, NJ). The V1 to V5 region of gp120 was amplified from the viral DNA or RT products by *Taq* DNA polymerase (Qiagen) with primers ED5 and ED12 or ES7 and ES8 as previously described (16). PCR products were cloned with the TOPO TA cloning kit (Invitrogen) per the manufacturer's instructions, followed by direct automated sequencing of cloned gp120 amplicons (Genewiz, South Plainfield, NJ). Nucleotide sequences were aligned with ClustalX (36) and edited manually using BioEdit V7.0.9. A phylogenetic tree was constructed using the maximum likelihood method, and bootstrap values were generated with 1,000 repetitions.

**Sequence-specific PCR.** For detection of the Δ22-25 V3 sequence, plasma cDNA products were subjected to PCR using Hot Star *Taq* DNA polymerase with primers V3-del (5′-AATTAAAACTGTGCATTACAA-3′) and WR8 (5′-CGGGGAGAGCATTTTACATA-3′) using the following cycling conditions: 95°C for 10 min followed by 35 cycles of 95°C for 30 s, 57.5°C for 20 s, and 72°C for 20 s and final extension at 72°C for 10 min. The sensitivity of the detection assay for Δ22-25 V3 sequence was 1 variant copy among $10^4$ R5 targets. For detection of RRW/RRW.A V3 sequences, primers SH85 (5′-AAAAGTATACATATAAGAAGGT-3′) and V3-OAS (5′-CAGTAGAAAAATTCCCCTCCACA-3′) were used with the following cycling profile: 95°C for 10 min followed by 35 cycles of 95°C for 30 s, 47.7°C for 20 s, and 72°C for 20 s, with the final extension at 72°C for 10 min. The sensitivity of detection for RRW/RRW.A was 1 variant copy among $10^6$ R5 targets. Amplified products were visualized by electrophoresis in ethidium bromide (EtBr)-stained 2% agarose gels.

**Plasmid constructs and pseudotype virus production.** The generation of DG08 Env expression plasmids and luciferase-reporter viruses has been described previously (43). For expression of CA28 envelope glycoproteins, full-length gp160 coding sequence was amplified from RT products with primers SH43 (5′-AAGACAGAATTCATGAGAGTGAAGGGGATCAGGAAG-3′) and SH44 (5′-AGAGAGGGATCCTTATAGCAAAGCCCTTTCAAAGCCCT-3′) and subcloned into the pCAGGS vector. To generate luciferase reporter viruses capable of only a single round of replication, an envelope *trans*-complementation assay was used as previously described (12). Briefly, Env expression plasmid and the NL4.3LucE-R- vector were cotransfected by polyethyleneimine (PEI) (Polyscience, Warrington, PA) into $2.5 \times 10^6$ 293T cells plated in a 100-mm plate. Cell culture supernatants were harvested 72 h later, filtered through 0.45-μm-pore-size filters, and stored at −70°C in 1-ml aliquots. Pseudoviruses were quantified for p24gag content (Beckman Coulter, Fullerton, CA).

**Determination of entry efficiency and coreceptor usage.** For assessment of entry efficiency and coreceptor usage of reporter viruses, $7 \times 10^3$ TZM-bl, U87.CD4.CCR5, or U87.CD4.CXCR4 cells were seeded in 96-well plates 24 h before use and infected, in triplicate, with 3 ng p24gag equivalent of the indicated pseudovirions followed by incubation for 72 h at 37°C. At the end of the incubation period, the cells were harvested, lysed, and processed for activity according to the manufacturer's instructions (Luciferase Assay System; Promega, Madison, WI). Entry, as quantified by luciferase activity, was measured with an MLX microtiter plate luminometer (Dynex Technologies, Inc., Chantilly, VA). For the entry blocking assays, U87.CD4 indicator cells were pretreated with 4-fold serial dilutions of TAK-779, PSC-RANTES, or AMD3100 for 30 min at 37°C before

infection. The cells were lysed after 72 h of incubation at 37°C and processed for β-galactosidase activity (Galacto-Star system; Applied Biosystems, Bedford, MA). The percentage of entry blocking was calculated by the amount of entry in the presence of the inhibitor relative to that in the absence of the inhibitor, and 50% inhibitory concentration ($IC_{50}$) was determined using the Prism 4 software (GraphPad, San Diego, CA).

**Statistical analysis.** Analysis of $IC_{50}$ comparing two groups was performed by the Mann-Whitney U test and considered statistically significant at $P < 0.05$.

## RESULTS

**V3 loop deletion variants predominate at the time of first X4 appearance in macaque CA28.** To further extend our understanding of the spectrum of variants present at the time of coreceptor switch in R5 $SHIV_{SF162P3N}$-infected macaques, we investigated the transitional intermediates in CA28. The envelope (Env) V1-V5 sequence of circulating viruses in this animal at 11 wpi, a time corresponding to the earliest detection of X4 variants bearing the signature V3 RRW.A mutations by sequence-specific PCR, was determined. Surprisingly, clonal sequence analysis revealed that 34 of 38 Env clones amplified from plasma of CA28 at this time had four amino acid deletions in the C terminus of the V3 loop (Δ22-25) that increased the net charge of this domain to +6 (Fig. 1A). Of the remaining clones, three had wild-type (WT) sequence, while one harbored mutations in the V3 loop that changed the GPG crown loop sequence to RRW but with the downstream alanine residue intact. This RRW V3 mutant was also a minor Env variant in the PBMC (3 of 70 clones sequenced), with 21 of 70 clones in this blood compartment harboring the V3 deletion sequence and with the majority (>60%) containing WT sequence. At the time of necropsy 4 weeks later, however, the Δ22-25 V3 deletion mutant now represented a minor population in the plasma of CA28 (4 of 31 clones sequenced) and was undetectable in the PBMC. The RRW-bearing V3 variants were also undetectable among over 30 clones sequenced from the plasma and PBMC of CA28 at necropsy. Instead, 1 of 31 plasma envelope clones had the signature X4 RRW.A V3 loop motif. Sequence-specific PCR analysis on plasma of CA28 showed that the Δ22-25 V3 loop variant could be detected as early as 9 wpi, 2 weeks prior to the detection of RRW- and RRW.A-bearing variants in this animal (Fig. 1B).

The poor representation of the signature X4 RRW.A V3 loop sequences in the blood of macaque CA28 at the time of necropsy (15 wpi) prompted us to examine their presence in tissue sites. This is because previous observations in macaques BR24 and DG08 suggested that peripheral lymph nodes (LNs) are the preferred sites of X4 evolution and amplification (43, 54). The results showed ready detection of the signature X4 RRW.A sequence in the axillary (35%), iliac (19%), and inguinal (20%) LN but not in the gut (intraepithelial lymphocytes [IEL] or lamina propria lymphocytes [LPL]) or in intestinal LNs such as the colonic and mesenteric LN (Fig. 1C). The RRW-bearing V3 variants, however, could not be detected in any of the tissue sites examined by clonal analysis at end-stage disease. In contrast, the Δ22-25 deletion variant has a much wider tissue distribution, detectable in both the gut and lymph nodes, particularly in the colonic LN, where 14 of 14 clones sequenced contained this V3 motif. The finding of signature X4 V3 sequences in peripheral lymph nodes and not in the gut (IELs and LPLs) of macaque CA28 is in agreement with previous observations in macaques BR24 and DG08, lending further support for secondary LNs as the preferred sites of X4 virus emergence and expansion. Furthermore, the wider distribution and greater representation of the Δ22-25 V3 variant in tissue sites are consistent with its emergence and expansion prior to that of the RRW and RRW.A mutant viruses in CA28.

**Distinct dualtropic variants coexist in macaque CA28.** The Δ22-25 V3 variant in CA28 harbors the same V3 deletion sequence that has been shown to confer CXCR4 usage to a variant in macaque DG08 which retained and preferred CCR5 for entry (Table 1). To determine coreceptor usage of the Δ22-25 as well as the RRW V3 mutants in CA28, full-length gp160 envelopes (Envs) were amplified and used in the generation of pseudotyped reporter viruses for infectivity studies. To enhance our chances of obtaining these variant envelopes, especially those with RRW mutations which are present at extremely low levels, viruses recovered from peripheral blood of CA28 at 15 wpi were used as a source for amplification. We find that the proportions of these underrepresented variants increased with low-passage propagation of plasma- or PBMC-associated viruses (data not shown). Pseudoviruses expressing WT and X4 RRW.A Envs amplified from propagated viruses were also obtained and served as coexisting R5 and X4 viruses, respectively. As expected, pseudoviruses expressing WT Env infected U87.CD4.CCR5 but not U87.CD4.CXCR4 cells, whereas the RRW.A-bearing virus showed the opposite phenotype, infecting U87.CD4.CXCR4 but not U87.CD4.CCR5 cells (Fig. 2A). The Δ22-25 V3 mutant in CA28 could infect U87.CD4 cells expressing either CCR5 or CXCR4, while viruses expressing Envs with the RRW V3 mutation, similar to the RRW.A-bearing variants, infected U87.CD4.CXCR4 but not U87.CD4.CCR5 cells.

To investigate coreceptor preference of the Δ22-25 virus in CA28, blocking experiments with CCR5 and CXCR4 antagonists in TZM-bl cells that express both coreceptors were performed. The results confirmed the coreceptor preference of viruses pseudotyped with WT or RRW.A V3 loop-bearing envelopes (Fig. 2B). Infection with WT V3 pseudovirus was blocked with the CCR5 inhibitor TAK779 but not with the CXCR4 inhibitor AMD3100, while the converse was observed for viruses containing RRW.A mutations in the V3 loop. Infection of TZM-bl cells with pseudovirus expressing the Δ22-25 V3 sequence was blocked to a greater extent by TAK779 (56%) than by AMD3100 (25%). Thus, similar to the Δ22-25 V3 variant in DG08 (Table 1), this Env variant in CA28 could function with CXCR4 but showed a preference for CCR5 usage and could be classified as dual-R as well. Interestingly, while AMD3100 efficiently blocked infection of TZM-bl cells with the RRW pseudovirus (70%), partial inhibition was also seen with TAK779 for this virus (26%). Dualtropic HIV-1 variants that use CXCR4 more efficiently than CCR5 have also been reported (30), and in this respect, the RRW variant in CA28 could be designated dual-X. Table 2 summarizes the transitional intermediates identified in CA28, showing a spectrum of dualtropic phenotypes similar to those seen in HIV-1-infected individuals.

To examine the evolutionary relationship of the transitional intermediates in macaque CA28, neighbor-joining tree analysis of Env V1-V5 sequence was performed. The results showed that while the dual-X RRW- and X4 RRW.A-bearing se-

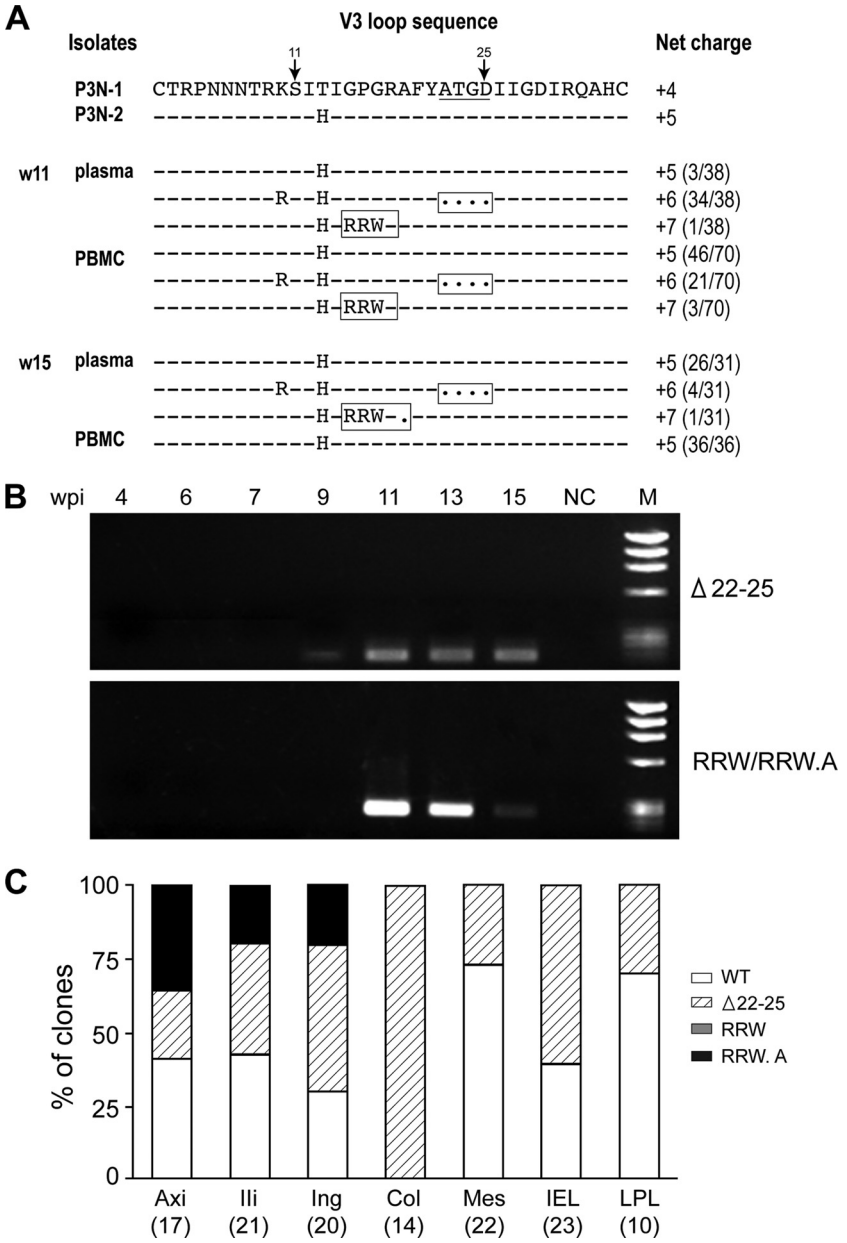


FIG. 1. Infecting virus population in macaque CA28 during coreceptor switch. (A) V3 loop sequence comparison of representative $SHIV_{SF162P3N}$ clones (P3N-1, P3N-2) and week (w)11 and w15 plasma and PBMC viruses in macaque CA28. Dots indicate gaps, dashes stand for identity in sequences, and the net positive charge of this region is shown on the right. Positions 11 and 25 within the V3 loop are indicated by arrows, and the 4-amino-acid deletion is underlined in the reference sequence. The numbers in parentheses represent the numbers of clones matching the indicated sequence per total number of clones sequenced. Amino acid residues predicted to confer CXCR4 usage are boxed. (B) Tracking the emergence of RRW/RRW.A- and Δ22-25-bearing variants in plasma using sequence-specific PCR. wpi, week postinfection; NC, negative control using plasma from an uninfected macaque; M, marker. (C) Distribution of V3 variants in tissue compartments of macaque CA28 at time of necropsy as determined by clonal sequence analysis. Numbers in parentheses indicate numbers of gp120 clones sequenced from each of the tissue sites. Ing, inguinal LN; Mes, mesenteric LN; Axi, axillary LN; Ili, iliac LN; Col, colonic LN; IEL, intraepithelial lymphocyte; LPL, lamina propria lymphocyte from the jejunum.

quences clustered together on the tree, they sat on branches that differed from those of the dual-R Δ22-25-bearing sequences (Fig. 3). These findings in CA28 therefore are consistent with those in DG08 (43), supporting the notion that multiple switch events leading to the emergence of diverse tropism variants can evolve in parallel in macaques infected with R5 $SHIV_{SF162P3N}$.

**Change in dominance of tropism variants during the course of coreceptor switching in R5 $SHIV_{SF162P3N}$-infected macaques.** Clonal Env sequence analysis of variants in tissues obtained from macaque DG08 at the time of first X4 appearance (13 wpi) and at end-stage disease (20 wpi) suggested that while the dual-R Δ22-25 switch preceded the X4 HR switch event temporally, its presence diminished over time, implying a

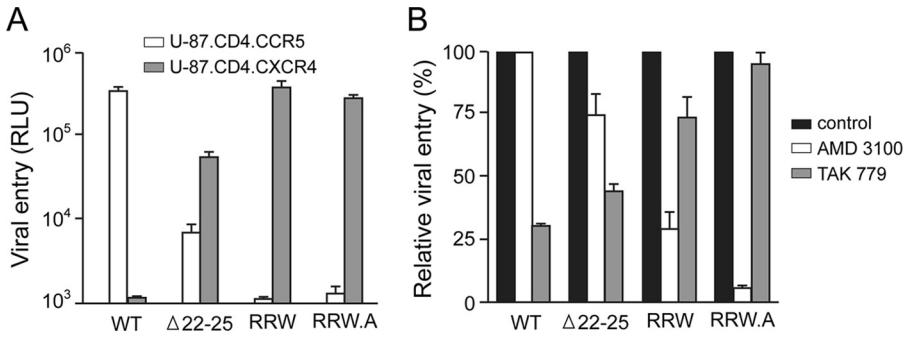


FIG. 2. Coreceptor usage (A) and preference (B) of V3 variants in CA28. Relative entry of pseudotyped reporter viruses in U87.CD4.CCR5 and U87.CD4.CXCR4 indicator cells was determined (A), and blocking of entry in TZM-bl cells with 1 μM CCR5-specific (TAK779) and CXCR4-specific (AMD3100) inhibitors was performed to determine coreceptor preference of the reporter viruses (B). Data are the means and standard deviations of results from triplicate wells and are representative of at least two independent experiments. RLU, relative light units.

loss of competitive fitness (43). Clonal Env sequences of viruses in longitudinal plasma and PBMC samples from DG08 confirmed this change in dominance of the V3 loop variant (Fig. 4). Of 44 plasma Env clones amplified at 13 wpi, 34% had an ATGD deletion in the V3 loop, with the remaining being WT, but over 97% of the 41 clones sequenced 1 week later harbored this mutation. Dominance of the Δ22-25 V3 variant also increased in PBMC within this same time period, from 17% to 98%. Notably, the remaining clone sequenced at 14 wpi in the PBMC compartment had insertions of histidine and isoleucine (HI) upstream of the GPG crown. Variants bearing these V3 insertions had been shown to be the evolutionary, functional, and antigenic intermediates of the HR-bearing X4 virus in macaque BR24 (27, 54). At the time of necropsy 6 weeks later (20 wpi), the dual-R Δ22-25 V3 was present at much lower frequency in the PBMC (3.5%) and not at all in the plasma, while variants with HI insertions could not be detected in either compartment. However, the dual-R Δ22-25 variant was present in both PBMC (16%) and plasma (3.3%) 2 weeks prior to necropsy (18 wpi), and variants with the signature X4 HR insertions could be detected in PBMC (13%) but not in the plasma at this time point. The transitory nature of the HI variant in DG08 and its detection prior to that of the HR variant in PBMC suggest that, as with macaque BR24, it also could be the R5X4 transitional intermediate of the HR-bearing X4 virus in this macaque (Table 2).

The dynamics in the change in dominance of the V3 tropism variants was similar in macaque CA28. Although sequence-specific PCR showed that the Δ22-25 variant first emerged in the plasma at 9 wpi (Fig. 1B), none of the 17 PBMC and 23 plasma Env clones sequenced at this time point harbored this deletion, suggesting that it is present at <5% frequency. Two weeks later, however, this variant represented ~90% and 30% of the plasma and PBMC envelope clones sequenced, respectively. The frequency of the Δ22-25 V3 variant continued to increase in PBMC but dropped to 15% in the plasma at 13 wpi. At the time of necropsy, however, the Δ22-25 V3 variants could not be found in 36 PBMC clones sequenced but maintained the same representation in the plasma. The dual-X RRW-bearing variant was present at low frequencies (<4%) in both the plasma and PBMC at 11 and 13 wpi but was undetectable at the time of necropsy. Instead, variants bearing the signature X4 RRW.A sequence now appeared in the plasma, albeit at low frequencies (~3%). These changes in virus population in the two macaques during and following the time of first X4 appearance prompted us to examine the underlying basis.

**Differences in fitness of the dualtropic transitional intermediates contribute to the change in infecting virus population during coreceptor switching in macaques CA28 and DG08.** To determine if fitness disadvantage of the dual-R Δ22-25 variant explains its diminished dominance with time, the entry efficiency and sensitivity of the V3 variants in macaques DG08 and CA28 to CCR5 as well as CXCR4 inhibitors were determined and compared, with sensitivity to the inhibitors serving as surrogate markers for coreceptor utilization efficiencies. We were not able to obtain functional HI-bearing gp160 from DG08 for these analyses, however, because of its transitory nature and extremely low frequency. The results showed differences in infection of TZM-bl cells that likely reflect differences in the Envs to interact with target cells. For DG08, entry

TABLE 2. Summary of transitional intermediates identified in this study[a]

| Macaque | Variant | Time of emergence | CD4 T-cell count[b] | V3 loop sequence | Tropism |
|---|---|---|---|---|---|
| CA28 | Δ22-25 | 9 wpi | 585 | CTRPNNNTRRSIHI..GPGRAFY....IIGDIRQAHC | Dual-R |
| | RRW | 11 wpi | 237 | ---------K----..**RRW**----ATGD---------- | Dual-X |
| DG08 | HI | 13 wpi | 314 | ---------K--R-**HI**-------ATGD---------- | R5X4[c] |

[a] wpi, weeks postinfection. For V3 sequence, dots indicate gaps and dashes stand for identity in sequences. Amino acid residues predicted to confer CXCR4 usage are in bold type.
[b] CD4 T cell count (per μl blood) at time of tropism variant emergence.
[c] Variants with HI insertions in the V3 loop had been previously shown to be dualtropic (see Table 1).

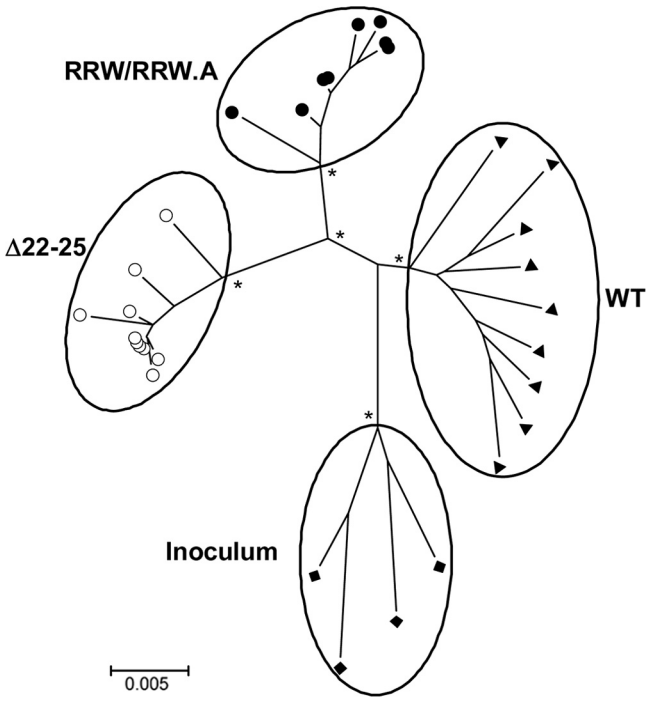


FIG. 3. Phylogenetic tree showing the relationship between Env variant sequences (V1 to V5) in macaque CA28. A neighbor-joining tree rooted on four functional sequences of the inoculating virus $SHIV_{SF162P3N}$ was generated. The scale bar indicates the genetic distance along the branches in nucleotides, and the asterisk at the node represents a bootstrap value of >70%. ◆, representative clones in the inoculum; ▲, WT variants; ●, RRW/RRW.A-bearing variants; ○, Δ22-25-bearing variants.

of the Δ22-25 and HR V3 variants was less efficient than those of the coevolving WT viruses, with the Δ22-25 variant being the most inefficient (WT>HR>Δ22-25) (Fig. 5A). Moreover, the dual-R Δ22-25 virus in DG08 used CCR5 less efficiently than the coevolving WT viruses (Fig. 5A), as reflected by lower concentrations of the CCR5 inhibitors TAK779 and PSC-RANTES required to inhibit 50% of infection ($IC_{50}$) with this virus than with the WT virus in U87.CD4.CCR5 cells. However, the difference did not reach statistical significance. The dual-R Δ22-25 virus, however, was significantly less efficient in engaging CXCR4 than the X4 HR variant ($P = 0.0495$). Similar observations were made with the CA28 viruses (Fig. 5B). Compared to results for the coevolving WT virus, entry into TZM-bl cells of all the V3 loop mutants was attenuated, with the following rank order of efficiency: WT > RRW.A > RRW > Δ22-25 V3 mutants. Furthermore, the dual-R Δ22-25 virus in CA28 was significantly less efficient in using the CCR5 coreceptor than the coevolving WT virus ($P = 0.0209$ and $P = 0.0495$ for TAK779 and PSC-RANTES, respectively). It was also significantly less efficient in using CXCR4 than the dual-X RRW ($P = 0.0433$) and the X4 RRW.A ($P = 0.0209$) viruses. We noted that while the dual-R viruses in DG08 and CA28 harbored the same V3 deletions, the V3 mutant in CA28 was less efficient in using CCR5 as well as CXCR4 than the variant in DG08, suggesting that a region(s) outside the V3 loop modulates coreceptor usage efficiency. Regardless, the results show that the dual-R Δ22-25 variant in both CA28 and DG08 is at a disadvantage in entry and in engaging CCR5 and CXCR4 compared to the coevolving R5, dual-X, and X4 viruses. Furthermore, the observations that the RRW-bearing virus still retains residual CCR5 engaging ability (Fig. 2C) and is genetically linked to but uses CXCR4 less efficiently than the final X4 RRW.A virus suggest that it serves as an intermediate in this pathway of tropism switch.

## DISCUSSION

In this study, we tested the hypothesis that the fitness of the transitional intermediates plays a role in determining their dominance and that this, in turn, impacts the composition of the virus population during coreceptor switching in R5

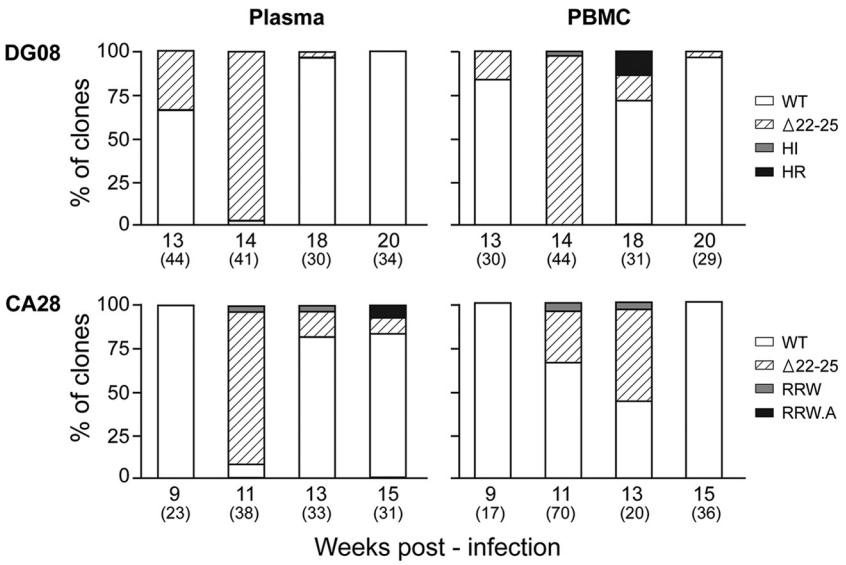


FIG. 4. Distribution of V3 variants in plasma and PBMC of macaques DG08 and CA28 over time. Numbers in parentheses indicate numbers of Env clones sequenced at indicated time points.

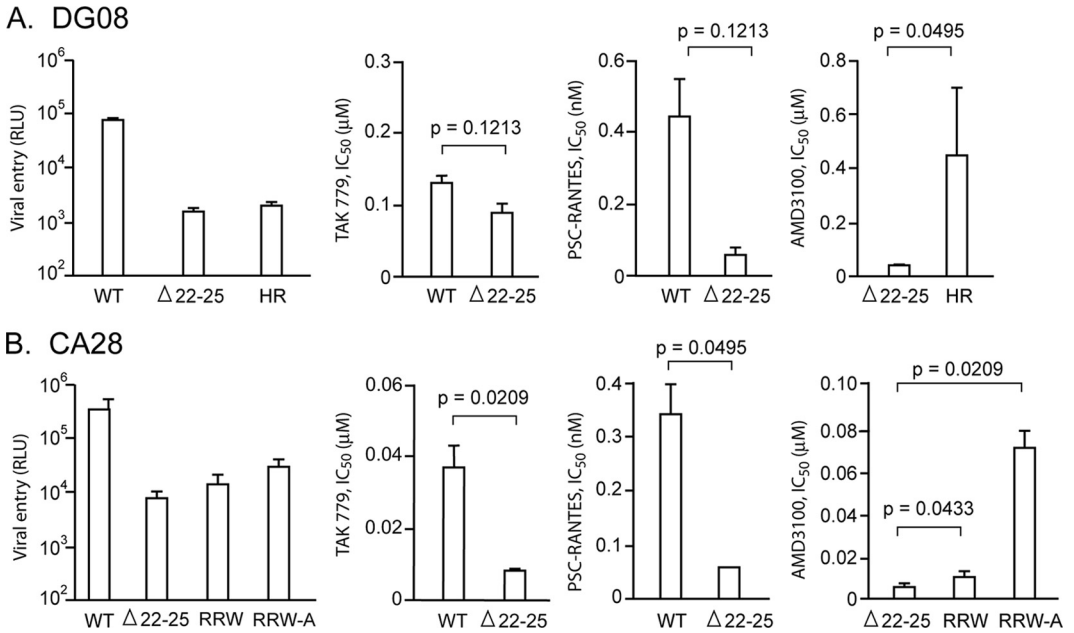


FIG. 5. Entry and coreceptor usage efficiencies of V3 variants in macaques DG08 (A) and CA28 (B). Determination of relative entry of pseudotyped reporter viruses in TZM-bl cells and blocking of pseudovirions with increasing concentrations of the CCR5 inhibitors TAK779 and PSC-RANTES and the CXCR4 inhibitor AMD3100 were performed. 50% inhibitory concentrations ($IC_{50}$) of the inhibitors were determined using Prism 4 software (GraphPad, San Diego, CA). RLU, relative light units. Data shown are means ± standard errors of the mean of results of at least two to four independent experiments.

$SHIV_{SF162P3N}$-infected macaques. We find that a spectrum of dualtropic viruses coexist in macaques CA28 and DG08, with a variant harboring four amino acid deletions in the V3 loop (Δ22-25) that preferred CCR5 over CXCR4 use dominant in both at the time of first X4 virus detection. With the emergence of viruses that used exclusively CXCR4, or used CXCR4 better than CCR5, dominance of the Δ22-25 V3 variant waned. The Δ22-25 viruses in CA28 and DG08 were less efficient in viral entry and in engaging the CCR5 and CXCR4 coreceptors than the coevolving WT and X4 viruses, respectively, suggesting that they are at a fitness disadvantage. Collectively, our data demonstrate successive changes in the infecting virus population during the process of coreceptor switch in both macaques, with a preference for X4 viruses with higher coreceptor usage efficiency. Moreover, these observations support our hypothesis that although the dual-R Δ22-25 virus had an advantage over earlier or coevolving R5 viruses when it first appeared because of target cell expansion through acquisition of CXCR4 usage, this advantage was lost with the subsequent emergence of viruses that used CXCR4 better, accounting for its diminished dominance with time.

We find that some of the same sequence motifs conferring CXCR4 usage have occurred in different infected animals: for example, HR and HI V3 insertions in macaques BR24 and DG08 (Tables 1 and 2), Δ22-25 V3 deletion in CA28 and DG08 (Tables 1 and 2), and RRW in CA28 and macaque DG88 (data not published). These X4 motifs were not present in over 10,000 V3 sequences obtained from the $SHIV_{SF162P3N}$ inoculum by ultra-deep sequencing (unpublished data), suggestive of convergent evolution. Indeed, convergent envelope evolution has previously been reported in SIV RPs, with substitutions concentrated in the V2 and V3 domains (14, 44). The parallels in the molecular evolutionary processes leading to the expansion or switch to CXCR4 use of the R5 $SHIV_{SF162P3N}$ isolate in the different rapid-progressing infected macaques suggest similar selective pressures for and limited pathways to coreceptor switch of this virus. Constraints in the ability of HIV-1 to mutate in response to immune pressures have been reported (2). However, since immune selection pressures are lacking or diminished in RP monkeys, this is unlikely to be a major factor in restricting the R5-to-X4 mutational changes in these animals. Structural constraints in accommodating amino acid changes required for CXCR4 usage have been suggested to limit the pathways available for coreceptor switching (39, 42). Specifically, requirements of inserting charged amino acids at specific locations within envelope gp120 and strong bias in favor of G-to-A substitutions rather than random mutations have been reported to impede coreceptor switching *in vitro* (42). Substitutions that generated the charged amino acid His or Arg are found in the V3 loop of macaques with coreceptor switch (Tables 1 and 2). Whether APOBEC3G, the cellular cytosine deaminase whose function is antagonized by viral Vif expression (48), and other host innate restriction factors also play roles in restricting the mutational pathways to coreceptor switch *in vivo* requires further investigation.

Variants with V3 loop deletions are the earliest X4 virus to emerge in both CA28 and DG08. Consistent with *in vitro* data showing that genetic truncation of the V3 loop is typically associated with significant loss of CCR5 utilization and Env function (10, 23, 35, 45, 59, 61), these V3 loop deletion mutants are less fit. So what host selective pressure(s) favors their early emergence *in vivo*? In addition to being a principal determinant of tropism, the V3 loop acts as an immunological shield, protecting a conserved envelope region(s) that would other-

wise be a target for neutralizing antibodies (26, 41). Indeed, truncation of the V3 loop has been shown to enhance sensitivity to neutralization with monoclonal antibodies (MAbs) directed to the CD4 and coreceptor binding sites (10, 35, 45, 59–61). Moreover, the loss of CCR5 interaction of V3 loop-deleted Envs can be compensated for by adaptive mutations in gp120 that enhanced use of CD4 (1). We find that the Δ22-25 V3 variants are highly sCD4 sensitive (data not shown), suggestive of exposure of the CD4 binding site and better CD4 usage. Furthermore, their emergence is at a time when the CD4 T cell count is above 300 cells per μl blood (Tables 1 and 2), implying that $CD4^+$ T cell limitation is not the selection factor for viruses to expose their CD4 binding site to increase CD4 binding. Thus, it is tempting to speculate that an early selective pressure to which viruses in the R5 $SHIV_{SF162P3N}$-infected RPs are subjected is the need to bind CD4 better to infect target cells that express small amounts of the receptor. As neutralization antibody selective pressure is absent or diminished in the RPs, increased CD4 binding may be best achieved by shortening of the V3 loop to expose the receptor binding site. Furthermore, although the truncation comes with a cost to replication fitness, the mutation is fixed and selected for because the conformational change associated with the V3 deletion also conferred CXCR4 use, expanding the target host cells that can be infected by the virus. This hypothetical mechanistic model for coreceptor switch in macaques CA28 and DG08 merits further investigation.

The rare presence of the X4 HR and RRW.A viruses by clonal analysis in the blood and gut of macaques CA28 and DG08 at end-stage disease contrasts with their ready detection in superficial external (axillary and inguinal) as well as internal (e.g., iliac) lymph nodes. Similar findings of the presence of syncytium-inducing HIV-1 in lymph nodes but not in peripheral blood have previously been reported in infected individuals at the time of death (37, 53). In this regard, it has been shown that lymphoid tissue in the gut is the principal site of HIV-1/SIV replication *in vivo* (5, 24, 25, 38, 40, 57). Furthermore, while $CD4^+$ T cells account for >90% of the viral load during early virus infection, macrophages may contribute substantially to plasma viral load during late-stage infection (19, 29, 32, 40). On a per-cell basis, productively infected macrophages cumulatively release at least 10-fold more viruses than do productively infected T cells (18), and macrophages generate virions with greater levels of infectivity than T cells (21). Moreover, they are the primary virus-producing cells following the nearly complete depletion of $CD4^+$ target T cells in SIV-infected rapid progressors (6). Macaque DG08 was diagnosed with SIV encephalitis (unpublished observations), and macrophages were found to be the principal SHIV-infected cells at end-stage disease in CA28 (unpublished data). As R5 viruses are more efficient in infection of macrophages than X4 viruses (50, 62), this then could explain the lower representation of X4 variants in the plasma than in lymph node compartments of HIV-1-infected individuals and R5 SHIV-infected macaques at the time of death. It will be of interest to compare macrophage tropism of coevolving R5, dualtropic, and X4 viruses in CA28 and DG08.

In summary, we show that multiple pathways for expansion to CXCR4 usage coexist in R5 $SHIV_{SF162P3N}$-infected macaques, with fitness of the transitional intermediates playing a role in determining their outgrowth and, consequently, the pathway for phenotypic switch. Entry and coreceptor usage efficiencies of the transitional intermediates were lower than that of the coevolving WT virus, supporting the notion that fitness disadvantage is a blockade to X4 virus emergence and expansion *in vivo*. The same sequence motifs conferring CXCR4 usage can be found in more than one animal, suggesting limited transitional pathways and similar selection pressures. Further characterization of the transitional intermediates, in particular the earliest CXCR4-using Δ22-25 V3 variants, with regard to susceptibility to neutralization with additional CD4 and coreceptor binding site antibodies, as well as their ability to infect target cells with low CD4 expression levels, such as primary macrophages, may uncover the specific selection forces that modulate the abundance of these and other tropism variants. It may also be of interest to conduct 454 deep sequencing of the V3 loop to detect rare or transient tropism intermediates in the infected animals to gain detailed insights into the multistep and gradual process of coreceptor switch *in vivo*.

## ACKNOWLEDGMENTS

We are grateful to the NIH AIDS Research and Reference Reagent Program, Division of AIDS, NIAID, NIH, for providing the following: the TZM-bl (catalog no. 8129 from John C. Kappes, Xiaoyun Wu, and Tranzyme, Inc.) and U87.CD4 (catalog no. 4035 and 4036 from HongKui Deng and Dan R. Littman) indicator cell lines and reagents TAK779 (catalog no. 4983 from Takeda Chemical Industries, Ltd.) and AMD3100 (catalog no. 8128 from AnorMed, Inc.). We thank Oliver Hartley for PSC-RANTES and Wendy Chen and Hiroshi Mohri for help with graphics and statistical analysis.

The work was supported by NIH grants RO1AI46980 and R37AI41945.

## REFERENCES

1. **Agrawal-Gamse, C., F. H. Lee, B. Haggarty, A. P. Jordan, Y. Yi, B. Lee, R. G. Collman, J. A. Hoxie, R. W. Doms, and M. M. Laakso.** 2009. Adaptive mutations in a human immunodeficiency virus type 1 envelope protein with a truncated V3 loop restore function by improving interactions with CD4. J. Virol. **83:**11005–11015.
2. **Allen, T. M., M. Altfeld, S. C. Geer, E. T. Kalife, C. Moore, M. O'Sullivan, K. I. Desouza, M. E. Feeney, R. L. Eldridge, E. L. Maier, D. E. Kaufmann, M. P. Lahaie, L. Reyor, G. Tanzi, M. N. Johnston, C. Brander, R. Draenert, J. K. Rockstroh, H. Jessen, E. S. Rosenberg, S. A. Mallal, and B. D. Walker.** 2005. Selective escape from CD8+ T-cell responses represents a major driving force of human immunodeficiency virus type 1 (HIV-1) sequence diversity and reveals constraints on HIV-1 evolution. J. Virol. **79:**13239–13249.
3. **Asjo, B., L. Morfeldt-Manson, J. Albert, G. Biberfeld, A. Karlsson, K. Lidman, and E. M. Fenyo.** 1986. Replicative capacity of human immunodeficiency virus from patients with varying severity of HIV infection. Lancet **ii:**660–662.
4. **Berger, E. A., P. M. Murphy, and J. M. Farber.** 1999. Chemokine receptors as HIV-1 coreceptors: roles in viral entry, tropism, and disease. Annu. Rev. Immunol. **17:**657–700.
5. **Brenchley, J. M., T. W. Schacker, L. E. Ruff, D. A. Price, J. H. Taylor, G. J. Beilman, P. L. Nguyen, A. Khoruts, M. Larson, A. T. Haase, and D. C. Douek.** 2004. CD4+ T cell depletion during all stages of HIV disease occurs predominantly in the gastrointestinal tract. J. Exp. Med. **200:**749–759.
6. **Brown, C. R., M. Czapiga, J. Kabat, Q. Dang, I. Ourmanov, Y. Nishimura, M. A. Martin, and V. M. Hirsch.** 2007. Unique pathology in simian immunodeficiency virus-infected rapid progressor macaques is consistent with a pathogenesis distinct from that of classical AIDS. J. Virol. **81:**5594–5606.
7. **Bunnik, E. M., E. D. Quakkelaar, A. C. van Nuenen, B. Boeser-Nunnink, and H. Schuitemaker.** 2007. Increased neutralization sensitivity of recently emerged CXCR4-using human immunodeficiency virus type 1 strains compared to coexisting CCR5-using variants from the same patient. J. Virol. **81:**525–531.
8. **Casper, C., L. Naver, P. Clevestig, E. Belfrage, T. Leitner, J. Albert, S. Lindgren, C. Ottenblad, A. B. Bohlin, E. M. Fenyo, and A. Ehrnst.** 2002. Coreceptor change appears after immune deficiency is established in chil-

dren infected with different HIV-1 subtypes. AIDS Res. Hum. Retroviruses **18:**343–352.
9. **Cheng-Mayer, C., D. Seto, M. Tateno, and J. A. Levy.** 1988. Biologic features of HIV-1 that correlate with virulence in the host. Science **240:**80–82.
10. **Chiou, S. H., E. O. Freed, A. T. Panganiban, and W. R. Kenealy.** 1992. Studies on the role of the V3 loop in human immunodeficiency virus type 1 envelope glycoprotein function. AIDS Res. Hum. Retroviruses **8:**1611–1618.
11. **Cocchi, F., A. L. DeVico, A. Garzino-Demo, A. Cara, R. C. Gallo, and P. Lusso.** 1996. The V3 domain of the HIV-1 gp120 envelope glycoprotein is critical for chemokine-mediated blockade of infection. Nat. Med. **2:**1244–1247.
12. **Connor, R. I., B. K. Chen, S. Choe, and N. R. Landau.** 1995. Vpr is required for efficient replication of human immunodeficiency virus type-1 in mononuclear phagocytes. Virology **206:**935–944.
13. **Connor, R. I., K. E. Sheridan, D. Ceradini, S. Choe, and N. R. Landau.** 1997. Change in coreceptor use correlates with disease progression in HIV-1-infected individuals. J. Exp. Med. **185:**621–628.
14. **Dehghani, H., B. A. Puffer, R. W. Doms, and V. M. Hirsch.** 2003. Unique pattern of convergent envelope evolution in simian immunodeficiency virus-infected rapid progressor macaques: association with CD4-independent usage of CCR5. J. Virol. **77:**6405–6418.
15. **De Jong, J. J., A. De Ronde, W. Keulen, M. Tersmette, and J. Goudsmit.** 1992. Minimal requirements for the human immunodeficiency virus type 1 V3 domain to support the syncytium-inducing phenotype: analysis by single amino acid substitution. J. Virol. **66:**6777–6780.
16. **Delwart, E. L., and C. J. Gordon.** 1997. Tracking changes in HIV-1 envelope quasispecies using DNA heteroduplex analysis. Methods **12:**348–354.
17. **Deng, H., R. Liu, W. Ellmeier, S. Choe, D. Unutmaz, M. Burkhart, P. DiMarzio, S. Marmon, R. E. Sutton, C. M. Hill, C. B. Davis, S. C. Peiper, T. J. Schall, D. R. Littman, and N. R. Landau.** 1996. Identification of a major co-receptor for primary isolates of HIV-1. Nature **381:**661–666.
18. **Eckstein, D. A., M. P. Sherman, M. L. Penn, P. S. Chin, C. M. De Noronha, W. C. Greene, and M. A. Goldsmith.** 2001. HIV-1 Vpr enhances viral burden by facilitating infection of tissue macrophages but not nondividing CD4+ T cells. J. Exp. Med. **194:**1407–1419.
19. **Embretson, J., M. Zupancic, J. L. Ribas, A. Burke, P. Racz, K. Tenner-Racz, and A. T. Haase.** 1993. Massive covert infection of helper T lymphocytes and macrophages by HIV during the incubation period of AIDS. Nature **362:**359–362.
20. **Fouchier, R. A., M. Groenink, N. A. Kootstra, M. Tersmette, H. G. Huisman, F. Miedema, and H. Schuitemaker.** 1992. Phenotype-associated sequence variation in the third variable domain of the human immunodeficiency virus type 1 gp120 molecule. J. Virol. **66:**3183–3187.
21. **Gaskill, P. J., M. Zandonatti, T. Gilmartin, S. R. Head, and H. S. Fox.** 2008. Macrophage-derived simian immunodeficiency virus exhibits enhanced infectivity by comparison with T-cell-derived virus. J. Virol. **82:**1615–1621.
22. **Glushakova, S., Y. Yi, J. C. Grivel, A. Singh, D. Schols, E. De Clercq, R. G. Collman, and L. Margolis.** 1999. Preferential coreceptor utilization and cytopathicity by dual-tropic HIV-1 in human lymphoid tissue ex vivo. J. Clin. Invest. **104:**R7–R11.
23. **Grimaila, R. J., B. A. Fuller, P. D. Rennert, M. B. Nelson, M. L. Hammarskjold, B. Potts, M. Murray, S. D. Putney, and G. Gray.** 1992. Mutations in the principal neutralization determinant of human immunodeficiency virus type 1 affect syncytium formation, virus infectivity, growth kinetics, and neutralization. J. Virol. **66:**1875–1883.
24. **Guadalupe, M., E. Reay, S. Sankaran, T. Prindiville, J. Flamm, A. McNeil, and S. Dandekar.** 2003. Severe CD4+ T-cell depletion in gut lymphoid tissue during primary human immunodeficiency virus type 1 infection and substantial delay in restoration following highly active antiretroviral therapy. J. Virol. **77:**11708–11717.
25. **Harouse, J. M., A. Gettie, R. C. Tan, J. Blanchard, and C. Cheng-Mayer.** 1999. Distinct pathogenic sequela in rhesus macaques infected with CCR5 or CXCR4 utilizing SHIVs. Science **284:**816–819.
26. **Hartley, O., P. J. Klasse, Q. J. Sattentau, and J. P. Moore.** 2005. V3: HIV's switch-hitter. AIDS Res. Hum. Retroviruses **21:**171–189.
27. **Ho, S. H., S. Tasca, L. Shek, A. Li, A. Gettie, J. Blanchard, D. Boden, and C. Cheng-Mayer.** 2007. Coreceptor switch in R5-tropic simian/human immunodeficiency virus-infected macaques. J. Virol. **81:**8621–8633.
28. **Ho, S. H., N. Trunova, A. Gettie, J. Blanchard, and C. Cheng-Mayer.** 2008. Different mutational pathways to CXCR4 coreceptor switch of CCR5-using simian-human immunodeficiency virus. J. Virol. **82:**5653–5656.
29. **Hockett, R. D., J. M. Kilby, C. A. Derdeyn, M. S. Saag, M. Sillers, K. Squires, S. Chiz, M. A. Nowak, G. M. Shaw, and R. P. Bucy.** 1999. Constant mean viral copy number per infected cell in tissues regardless of high, low, or undetectable plasma HIV RNA. J. Exp. Med. **189:**1545–1554.
30. **Huang, W., S. H. Eshleman, J. Toma, S. Fransen, E. Stawiski, E. E. Paxinos, J. M. Whitcomb, A. M. Young, D. Donnell, F. Mmiro, P. Musoke, L. A. Guay, J. B. Jackson, N. T. Parkin, and C. J. Petropoulos.** 2007. Coreceptor tropism in human immunodeficiency virus type 1 subtype D: high prevalence of CXCR4 tropism and heterogeneous composition of viral populations. J. Virol. **81:**7885–7893.
31. **Hwang, S. S., T. J. Boyle, H. K. Lyerly, and B. R. Cullen.** 1991. Identification of the envelope V3 loop as the primary determinant of cell tropism in HIV-1. Science **253:**71–74.
32. **Igarashi, T., C. R. Brown, Y. Endo, A. Buckler-White, R. Plishka, N. Bischofberger, V. Hirsch, and M. A. Martin.** 2001. Macrophage are the principal reservoir and sustain high virus loads in rhesus macaques after the depletion of CD4+ T cells by a highly pathogenic simian immunodeficiency virus/HIV type 1 chimera (SHIV): implications for HIV-1 infections of humans. Proc. Natl. Acad. Sci. U. S. A. **98:**658–663.
33. **Koot, M., I. P. Keet, A. H. Vos, R. E. de Goede, M. T. Roos, R. A. Coutinho, F. Miedema, P. T. Schellekens, and M. Tersmette.** 1993. Prognostic value of HIV-1 syncytium-inducing phenotype for rate of CD4+ cell depletion and progression to AIDS. Ann. Intern. Med. **118:**681–688.
34. **Kuiken, C. L., J. J. de Jong, E. Baan, W. Keulen, M. Tersmette, and J. Goudsmit.** 1992. Evolution of the V3 envelope domain in proviral sequences and isolates of human immunodeficiency virus type 1 during transition of the viral biological phenotype. J. Virol. **66:**4622–4627.
35. **Laakso, M. M., F. H. Lee, B. Haggarty, C. Agrawal, K. M. Nolan, M. Biscone, J. Romano, A. P. Jordan, G. J. Leslie, E. G. Meissner, L. Su, J. A. Hoxie, and R. W. Doms.** 2007. V3 loop truncations in HIV-1 envelope impart resistance to coreceptor inhibitors and enhanced sensitivity to neutralizing antibodies. PLoS Pathog. **3:**e117.
36. **Larkin, M. A., G. Blackshields, N. P. Brown, R. Chenna, P. A. McGettigan, H. McWilliam, F. Valentin, I. M. Wallace, A. Wilm, R. Lopez, J. D. Thompson, T. J. Gibson, and D. G. Higgins.** 2007. Clustal W and Clustal X version 2.0. Bioinformatics **23:**2947–2948.
37. **McGavin, C. H., S. A. Land, K. L. Sebire, D. J. Hooker, A. D. Gurusinghe, and C. J. Birch.** 1996. Syncytium-inducing phenotype and zidovudine susceptibility of HIV-1 isolated from post-mortem tissue. AIDS **10:**47–53.
38. **Mehandru, S., M. A. Poles, K. Tenner-Racz, A. Horowitz, A. Hurley, C. Hogan, D. Boden, P. Racz, and M. Markowitz.** 2004. Primary HIV-1 infection is associated with preferential depletion of CD4+ T lymphocytes from effector sites in the gastrointestinal tract. J. Exp. Med. **200:**761–770.
39. **Overbaugh, J., and C. R. Bangham.** 2001. Selection forces and constraints on retroviral sequence variation. Science **292:**1106–1109.
40. **Pantaleo, G., C. Graziosi, L. Butini, P. A. Pizzo, S. M. Schnittman, D. P. Kotler, and A. S. Fauci.** 1991. Lymphoid organs function as major reservoirs for human immunodeficiency virus. Proc. Natl. Acad. Sci. U. S. A. **88:**9838–9842.
41. **Pantophlet, R., and D. R. Burton.** 2006. GP120: target for neutralizing HIV-1 antibodies. Annu. Rev. Immunol. **24:**739–769.
42. **Pastore, C., A. Ramos, and D. E. Mosier.** 2004. Intrinsic obstacles to human immunodeficiency virus type 1 coreceptor switching. J. Virol. **78:**7565–7574.
43. **Ren, W., S. Tasca, K. Zhuang, A. Gettie, J. Blanchard, and C. Cheng-Mayer.** 2010. Different tempo and anatomic location of dual-tropic and X4 virus emergence in a model of R5 simian-human immunodeficiency virus infection. J. Virol. **84:**340–351.
44. **Ryzhova, E. V., P. Crino, L. Shawver, S. V. Westmoreland, A. A. Lackner, and F. Gonzalez-Scarano.** 2002. Simian immunodeficiency virus encephalitis: analysis of envelope sequences from individual brain multinucleated giant cells and tissue samples. Virology **297:**57–67.
45. **Saunders, C. J., R. A. McCaffrey, I. Zharkikh, Z. Kraft, S. E. Malenbaum, B. Burke, C. Cheng-Mayer, and L. Stamatatos.** 2005. The V1, V2, and V3 regions of the human immunodeficiency virus type 1 envelope differentially affect the viral phenotype in an isolate-dependent manner. J. Virol. **79:**9069–9080.
46. **Scarlatti, G., E. Tresoldi, A. Bjorndal, R. Fredriksson, C. Colognesi, H. K. Deng, M. S. Malnati, A. Plebani, A. G. Siccardi, D. R. Littman, E. M. Fenyo, and P. Lusso.** 1997. *In vivo* evolution of HIV-1 co-receptor usage and sensitivity to chemokine-mediated suppression. Nat. Med. **3:**1259–1265.
47. **Schuitemaker, H., M. Koot, N. A. Kootstra, M. W. Dercksen, R. E. de Goede, R. P. van Steenwijk, J. M. Lange, J. K. Schattenkerk, F. Miedema, and M. Tersmette.** 1992. Biological phenotype of human immunodeficiency virus type 1 clones at different stages of infection: progression of disease is associated with a shift from monocytotropic to T-cell-tropic virus population. J. Virol. **66:**1354–1360.
48. **Sheehy, A. M., N. C. Gaddis, J. D. Choi, and M. H. Malim.** 2002. Isolation of a human gene that inhibits HIV-1 infection and is suppressed by the viral Vif protein. Nature **418:**646–650.
49. **Shioda, T., J. A. Levy, and C. Cheng-Mayer.** 1991. Macrophage and T cell-line tropisms of HIV-1 are determined by specific regions of the envelope gp120 gene. Nature **349:**167–169.
50. **Simmons, G., J. D. Reeves, A. McKnight, N. Dejucq, S. Hibbitts, C. A. Power, E. Aarons, D. Schols, E. De Clercq, A. E. Proudfoot, and P. R. Clapham.** 1998. CXCR4 as a functional coreceptor for human immunodeficiency virus type 1 infection of primary macrophages. J. Virol. **72:**8453–8457.
51. **Simmons, G., D. Wilkinson, J. D. Reeves, M. T. Dittmar, S. Beddows, J. Weber, G. Carnegie, U. Desselberger, P. W. Gray, R. A. Weiss, and P. R. Clapham.** 1996. Primary, syncytium-inducing human immunodeficiency virus type 1 isolates are dual-tropic and most can use either Lestr or CCR5 as coreceptors for virus entry. J. Virol. **70:**8355–8360.
52. **Speck, R. F., K. Wehrly, E. J. Platt, R. E. Atchison, I. F. Charo, D. Kabat, B. Chesebro, and M. A. Goldsmith.** 1997. Selective employment of chemokine

receptors as human immunodeficiency virus type 1 coreceptors determined by individual amino acids within the envelope V3 loop. J. Virol. **71:**7136–7139.

53. **Tamalet, C., A. Lafeuillade, N. Yahi, C. Vignoli, C. Tourres, P. Pellegrino, and P. de Micco.** 1994. Comparison of viral burden and phenotype of HIV-1 isolates from lymph nodes and blood. AIDS **8:**1083–1088.
54. **Tasca, S., S. H. Ho, and C. Cheng-Mayer.** 2008. R5X4 viruses are evolutionary, functional, and antigenic intermediates in the pathway of a simian-human immunodeficiency virus coreceptor switch. J. Virol. **82:**7089–7099.
55. **Tersmette, M., J. M. Lange, R. E. de Goede, F. de Wolf, J. K. Eeftink-Schattenkerk, P. T. Schellekens, R. A. Coutinho, J. G. Huisman, J. Goudsmit, and F. Miedema.** 1989. Association between biological properties of human immunodeficiency virus variants and risk for AIDS and AIDS mortality. Lancet **i:**983–985.
56. **van't Wout, A. B., N. A. Kootstra, G. A. Mulder-Kampinga, N. Albrecht-van Lent, H. J. Scherpbier, J. Veenstra, K. Boer, R. A. Coutinho, F. Miedema, and H. Schuitemaker.** 1994. Macrophage-tropic variants initiate human immunodeficiency virus type 1 infection after sexual, parenteral and vertical transmission. J. Clin. Invest. **94:**2060–2067.
57. **Veazey, R. S., M. DeMaria, L. V. Chalifoux, D. E. Shvetz, D. R. Pauley, H. L. Knight, M. Rosenzweig, R. P. Johnson, R. C. Desrosiers, and A. A. Lackner.** 1998. Gastrointestinal tract as a major site of CD4+ T cell depletion and viral replication in SIV infection. Science **280:**427–431.
58. **Wei, X., J. M. Decker, S. Wang, H. Hui, J. C. Kappes, X. Wu, J. F. Salazar-Gonzalez, M. G. Salazar, J. M. Kilby, M. S. Saag, N. L. Komarova, M. A. Nowak, B. H. Hahn, P. D. Kwong, and G. M. Shaw.** 2003. Antibody neutralization and escape by HIV-1. Nature **422:**307–312.
59. **Wyatt, R., N. Sullivan, M. Thali, H. Repke, D. Ho, J. Robinson, M. Posner, and J. Sodroski.** 1993. Functional and immunologic characterization of human immunodeficiency virus type 1 envelope glycoproteins containing deletions of the major variable regions. J. Virol. **67:**4557–4565.
60. **Wyatt, R., M. Thali, S. Tilley, A. Pinter, M. Posner, D. Ho, J. Robinson, and J. Sodroski.** 1992. Relationship of the human immunodeficiency virus type 1 gp120 third variable loop to a component of the CD4 binding site in the fourth conserved region. J. Virol. **66:**6997–7004.
61. **Yang, Z. Y., B. K. Chakrabarti, L. Xu, B. Welcher, W. P. Kong, K. Leung, A. Panet, J. R. Mascola, and G. J. Nabel.** 2004. Selective modification of variable loops alters tropism and enhances immunogenicity of human immunodeficiency virus type 1 envelope. J. Virol. **78:**4029–4036.
62. **Yi, Y., S. Rana, J. D. Turner, N. Gaddis, and R. G. Collman.** 1998. CXCR-4 is expressed by primary macrophages and supports CCR5-independent infection by dual-tropic but not T-tropic isolates of human immunodeficiency virus type 1. J. Virol. **72:**772–777.